ANOVA Results (Methods)

Effect	Est. (wJC)	Sign.	Est. (CC)	Sign.
Intercept	56.21		63.18	
km	12.40	***	18.58	***
mm	-11.24	***	-22.69	***
hardcl	-1.33	n.s.	9.11	***
ng	11.61	***	19.73	***
cm	1.97	n.s.	-11.19	***
ufcl	-15.06	***	-7.63	***
som	0.97	n.s.	2.97	***
clara	1.32	n.s.	-17.09	***

***: <0.0001, **: <0.001, *: <0.05, n.s.: not significant

ANOVA Results (INC, CNR, NC)

Effect	Est. (wJC)	Sign.	Est. (CC)	Sign.
Intercept	56.21		63.18	
INC: 5	-23.87	***	-13.49	***
INC: 10	4.46	***	2.18	***
INC: 20	19.42	***	11.30	***
CNR: 1.33	-9.48	***	-7.71	***
CNR: 1.66	1.10	n.s.	1.50	*
CNR: 2.00	8.39	***	6.21	***
NC: artificial	2.68	***	7.18	***
NC: hybrid	-2.68	***	-7.18	***

***: <0.0001, **: <0.001, *: <0.05, n.s.: not significant

382

Functional magnetic resonance imaging (fMRI) for therapeutic monitoring of transcranial magnetic stimulation (TMS)

F. L. Giesel[1], A. Hempel[2], E. Hempel[3], T. Wuestenberg[4], U. Seidl[5], J. Schroeder[2], M. Essig[1]; [1]*Department of Radiology, German Cancer Research Center, Heidelberg, GERMANY,* [2]*Department of Psychiatry, University of Heidelberg, Heidelberg, GERMANY,* [3]*Department of Medical Engineering, Forschungszentrum Karlsruhe, Karslruhe, GERMANY,* [4]*Department of Neurology, Humboldt-University of Berlin, Berlin, GERMANY,* [5]*Department of Psychiatry, Universtiy of Heidelberg, Heidelberg, GERMANY.*

Introduction: Recent studies demonstrated acoustic hallucinations in patients with schizophrenia to be associated with activations in the superior temporal lobes. Based on the hypothesis of focal cortical inhibition low-frequency transcranial magnetic stimulation (TMS) was used, resulting in a slight reduction of hallucinations in some patients. In this case study functional magnetic resonance imaging was employed to image BOLD-effect changes in the temporal lobes under TMS-therapy.

Methods: In a curative attempt, a 30-year old schizophrenic patient (DSM-IV) with medication resistent acoustic hallucinations was treated with low-frequency TMS (fstim=1Hz) over a four week period. The TMS-effects were detected based on the auditory hallucinations rating scale. FMRI was performed in a 1.5 T clinical scanner (Magnetom Vision plus, Siemens, Erlangen, Germany) using the standard head coil and a GE-EPI sequence (volume of 30 slices, FOV 240 x 240 mm2, voxel size = 1,88 x 1,88 x 4 mm3, flip angle 90°, TR= 4.7 ms, TE 54 ms) using a design containing acoustic hallucinations. FMRI was performed prior to and after the TMS series to visualize possible cortical activation changes in the stimulated area. Data analyses were performed with SPM99 (http://fil.ion.ucl.ac.uk.spm). Activated voxels were identified by the General Linear Model approach for each condition.

Results: After the third week, the patient presented a reduced frequency of acoustic hallucinations of approx. 50%, while the loudness of the hallucinations remained unchanged over the 4 weeks of stimulation. FMRI demonstrated a BOLD-Effect activation reduction after TMS in speech related areas, which exceeded the local stimulation area.

Discussion: FMRI-data revealed an activation reduction in temporal and temporoparietal areas after TMS corresponding to the clinical recovery. The combination of TMS and functional imaging is promising, allowing an insight into neuro-biological mechanism during TMS intervention, which may help to improve technique and treatment success.

383

An educational tool for a better understanding of *k*-space through the reconstruction of magnetic resonance images

D. Moratal-Pérez[1], L. Martí-Bonmatí[2], M. E. Brummer[3], J. Millet-Roig[1], F. Castells[1], J. J. Rieta[1]; [1]*Ingeniería Electrónica, Universitat Politècnica de València, Valencia, SPAIN,* [2]*Radiology Department, Hospital Universitari Dr. Peset, Valencia, SPAIN,* [3]*Radiology Department, Emory University School of Medicine, Atlanta, GA.*

Introduction: In magnetic resonance imaging (MRI) the user has the control over how the data are acquired and how they can be manipulated in order to show the reconstructed image. Adjusting several parameters, the user can modify the spatial and temporal resolution, the field of view, the contrast, the speed of the acquisition, the influence of multiple artifacts and several other parameters that will contribute to create the final image.

The agent that makes this possible is known as *k*-space and it refers to the data matrix obtained directly from the magnetic resonance scanner before any kind of processing and before the application of the Fourier Transform, which will provide us of the reconstructed final image[1,2].

Materials and Methods: This tool has been developed using MATLAB R6.1 (Mathworks, Inc, Natick, MA). It has been created with a Graphical User Interface, in order to facilitate its use.

Results: The educational software tool that is introduced here tries to show in an intuitive and didactic way what happens to the reconstructed image associated to a *k*-space to which some basic processes –like low, high and band-pass filtering among others-have been applied. It offers also the possibility of adding noise or spikes in order to study the behaviour of the *k*-space and its associated image.

It is also possible, within this education tool, to learn how some basic reduced Field-of-View techniques like Rectangular Field-of-View and Half Fourier Imaging work, applying them to the *k*-space and observing how it is modified and so its associated image does.

Discussion/Conclusion:

This tool has been tested by radiologists achieving a high level of satisfaction and accomplishing its main **Objective:** to help to better understand the unknown concept of *k*-space and how the image is affected by modifying it.

It is interesting to remark that this educational software keeps in continuous growth.

References:

1. R. Mezrich, Radiology 1995, 195:297-315
2. D.B. Twieg, Med Phys 1983, 10(5):610-621

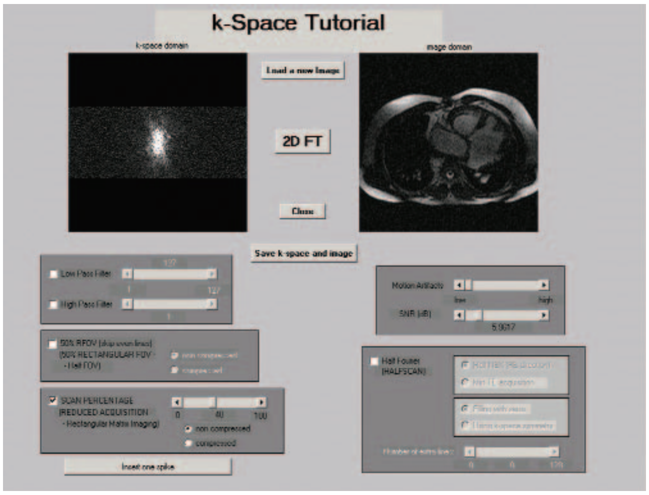

Figure 1. Main window of this *k*-space tutorial. At the upper part of the window we can see the *k*-space and its image associated to which all the desired operations will be applied. After having applied the desired operations, it is also possible to save the resulting image and its *k*-space.

384

Current concepts and applications for advanced image processing in MRI

H. von Tengg-Kobligk[1], K. T. Baudendistel[1], **J. T. Heverhagen**[1], M. J. McAuliffe[2], T. Kurc[3], J. H. Saltz[3], M. V. Knopp[1]; *[1]Department of Radiology, The Ohio State University, Columbus, OH, [2]Center for Information Technology, National Institutes of Health, Bethesda, MD, [3]Department of Biomedical Informatics, The Ohio State University, Columbus, OH.*

Purpose/Introduction: Advances in recent development of post processing equipment facilitate more elaborate image analysis on large data sets acquired using ultrafast MR, multi-slice CT, time dependent imaging data from these modalities, as well as ultrasound and nuclear medicine/PET imaging. The current PAC-Systems are not able to carry out the required functional image analysis. Most available analysis applications are being developed for a single specific purpose such as MR angiography, virtual colonoscopy, etc. In addition, radiological imaging is increasingly utilized for functional analysis and therapy monitoring applications requiring the assessment of multiple imaging studies. Currently, most clinical research groups focus on developing targeted applications for their specific needs without developing a generic infrastructure framework which then may be utilized for multiple modalities and applications.
Subjects and Methods: We present an implementation of a general image processing framework for MR image analysis and for the integration of other imaging modalities. The implemented heterogeneous PCs/Linux-based computing cluster uses modules developed in the programming languages IDL (Research Systems, Inc., Boulder, USA) and JAVA (Sun Microsystems, Inc., CA, USA). Developed applications are executed as pre-compiled run-time-modules which then can interface with third party imaging devices and workstations. Large scale computational image assessment for follow-up studies and computer-aided diagnosis was enabled by grid-enabled cluster computing capabilities.
Results: We identified, that all specific solutions have the following key components in common: image retrieval, image information database management, human interface, processing, quantification, visualization, communication of the findings, and archiving. A more automated workflow could be achieved by minimizing incompatibility issues due to propriertory image file formats and by introducing self written software for quality control and database managment. Vendor and modality independent processing was possible.
Discussion/Conclusion: This generic approach facilitated advanced image analysis and allows an effective integration of visualization and analysis tools into a PACS-oriented, radiological environment to improve research capabilities as well as clinical service.

385

White matter differences in autism: a voxel based morphometric study

G. D. Waiter[1], J. H. G. Williams[2], A. D. Murray[3]; *[1]Cognitive Neuroimaging Research Unit, School of Psychology, Mathematics and Computing Science, University of Aberdeen, Aberdeen, UNITED KINGDOM, [2]Department of Child Health, University of Aberdeen, Aberdeen, UNITED KINGDOM, [3]Department of Radiology, University of Aberdeen, Aberdeen, UNITED KINGDOM.*

Introduction: Autism(1) is a developmental disorder involving a wide variety of behavioural and cognitive abnormalities, with characteristic impairments in social communication. There is evidence for a genetic link(2) and also that pathologic mechanisms are in effect during the early stages of brain development(3). These factors suggest that structural differences may be present in the brain of subjects presenting with autism. This structural MRI study was conceived to test this hypothesis by imaging a group of young male adults with Autism with an age, IQ and handedness matched normal control group.
Methods: 16 young men diagnosed with Autism using ADI- revised (2000) and ADOS-G, were imaged. They were matched to 16 normal volunteers on age and IQ measured using either the WAIS-R or the WISC-R. Imaging was performed using a 1.5 T scanner (CVi, General Electric Medical Systems, Milwaukee, WI). A quadrature head coil was used to obtain high-resolution images using an SPGR sequence: FOV, 24cm; 20/6, (TR/TE); flip angle, 35^{o}; slices, 124; slice thickness, 1.6mm; matrix, 256x192; and in-plane resolution, 1 x 1 mm. A T1 template image was generated based on the average of all 32 participants. Preprocessing was based on the “Optimized VBM Protocol”(4) using SPM, with normalisation to the new group specific T1 template. Regionally specific differences in white matter between groups were assessed with an analysis of co-variance, with total brain volume as a nuisance variable. The resulting t-statistics were thresholded at $p=0.01$ (uncorrected) for display, and maxima at $p<0.005$ (uncorrected) are reported.
Results: Significant reduction in white matter volume was found throughout the brain with particular focus in the middle and posterior regions of the corpus callosum (CC), Fig. 1. No significant areas of increased white matter volume were found.